Structural Variation of Dinuclear Transition Metal Compounds with a Common Type of Ligand: Solid State and Solution Structures and Model Studies

Peter Comba,*[,1a] Sergey P. Gavrish,[1b] Robert W. Hay,[1c,d] Peter Hilfenhaus,[1a] Yaroslaw D. Lampeka,[1b] Philip Lightfoot,[1c] and Alexander Peters[1a]

Anorganisch-Chemisches Institut der Universität Heidelberg, Im Neuenheimer Feld 270, D-69120 Heidelberg, Germany, L. V. Pisarzhevskii Institute of Physical Chemistry of the National Academy of Sciences of the Ukraine, Prospekt Nauki 31, 252039 Kiew, Ukraine, and School of Chemistry, University of St. Andrews, Purdie Building, St. Andrews, Fife KY16 9ST, U.K.

Received June 23, 1998

The structural properties of the four-coordinate dinickel(II) and the (4 + 1)-coordinate dicopper(II) compounds of two bis(diamine-diamide) ligands, based on the condensation of 1,8-diamino-3,6-diazaoctane or ethane-1,2-diamine with bismalonic esters (that is the complexes of the bis-13-membered macrocyclic ligand L^1 and of the corresponding open-chained ligand L^2) are studied by X-ray crystallography, EPR spectroscopy, and molecular modeling. X-ray crystallography indicates that $Cu_2L^1(OH_2)_2$ and $Cu_2L^2(OH_2)_2$ have a stretched conformation (torsion angle $\phi(M-C_{bridgehead}-C'_{bridgehead}-M') = 180°$); Ni_2L^2 has the same stretched conformation, but Ni_2L^1 is folded ($\phi(M-C_{bridgehead}-C'_{bridgehead}-M') = 55°$). The dicopper(II) compounds have the same stretched structure in solution (MM-EPR), and molecular mechanics studies (strain energy as a function of the torsion angle ϕ) indicate that the most stable conformations are those observed in the solid state and in solution, i.e., stretched for $Cu_2L^1(OH_2)_2$, $Cu_2L^2(OH_2)_2$, and Ni_2L^2 and folded for Ni_2L^1. Reasons for the stabilization of the observed structures are discussed in detail.

Introduction

The coordination of macrocyclic ligands to metal ions is an efficient way to enforce particular, also uncommon and strained, coordination geometries and still obtain relatively stable products.[2] Therefore, macrocyclic ligand complexes have often been designed and prepared as low molecular weight model compounds for metalloproteins, where the rigid protein backbone enforces coordination geometries which are responsible for the selective activation of particular reaction channels. With an increasing amount of information on di- and multinuclear metalloproteins, the design, synthesis, and characterization of structural and spectroscopic model compounds, as well as the development of functional models for metal ion catalysis, are fast developing fields in coordination chemistry.[3]

A major problem in modeling multinuclear metalloproteins is to tune the distances between and the relative orientation of the chromophores.[3,4] In the present study we have tested the accuracy and viability of force field calculations to predict and interpret the structural features of bismacrocyclic and open-chained dinucleating ligand compounds of nickel(II) and copper(II).

The condensation of readily accessible bismalonic esters with polyamines is a relatively simple and versatile preparative method for the synthesis of dinucleating ligands.[5] With this scheme both the nature of the bridge between the two coordination sites and the coordination geometry may be widely varied. The condensation with diamines leads to open-chained bis(tetradentate) ligands,[6−8] and the reaction with polyamines yields bismacrocycles of various sizes and denticities.[9] Ligand molecules with directly linked subunits (e.g., L^1 and L^2, see Chart 1)[7a,b,8,9b,c] and derivatives with methylene,[9d] trimethylene,[6b,9a] *p*-xylylene,[7c] and other bridges[6a] have been described.

We report a detailed structural analysis of the dinickel(II) and the dicopper(II) compounds of L^1 and L^2, based on X-ray structural analyses of the solids, solution structural studies based on MM-EPR,[8,10] and conformational analyses based on molecular mechanics calculations.

* Corresponding author. E-mail: comba@akcomba.oci.uni-heidelberg.de.

(1) (a) Heidelberg. (b) Kiev. (c) St. Andrews. (d) Deceased January 8, 1999; with Bob we have lost a fine scientist and good friend.

(2) Comba, P. *Coord. Chem. Rev.* **1999**, *182*, 343.
(3) (a) Fenton, D. E.; Okawa, H. In *Perspectives on Bioinorganic Chemistry*; Hay, R. W., Dilworth, J. R., Nolan, K. B., Eds.; JAI Press Ltd.: London, 1993. (b) Karlin, K. D.; Tyeklar, Z.; Zuberbühler, A. D. In *Bioinorganic Catalysis*; Reedijk, J., Ed.; Marcel Dekker Inc.: New York, 1993. (c) Solomon, E. I.; Sundaram, U. M.; Machonkin, T. E. *Chem. Rev.* **1996**, *96*, 2563.
(4) (a) Fenton, D. E. In *Transition Metals in Supramolecular Chemistry*; Fabbrizzi, L., Poggi, A., Eds.; Kluwer Academic Publ.: Dordrecht, 1994. (b) Kaden, T. A. In *Transition Metals in Supramolecular Chemistry*; Fabbrizzi, L., Poggi, A., Eds.; Kluwer Academic Publ.: Dordrecht, 1994.
(5) Bradshaw, J. S.; Krakowiak, K. E.; Izatt, R. M. *Aza-Crown Macrocycles*; Wiley: New York, 1993.
(6) (a) Kimura, E.; Kuramoto, Y.; Koike, T.; Fujioka, H.; Kodama, M. *J. Org. Chem.* **1990**, *55*, 42. (b) Kodama, M. *Bull. Chem. Soc. Jpn.* **1995**, *68*, 2891.
(7) (a) Fabbrizzi, L.; Forlini, F.; Perotti, A.; Seghi, B. *Inorg. Chem.* **1984**, *23*, 807. (b) Buttafava, A.; Fabbrizzi, L.; Perotti, A.; Poggi, A.; Seghi, B. *Inorg. Chem.* **1984**, *23*, 3917. (c) Kido, H.; Takada, M.; Suwabe, M.; Yamaguchi, T.; Ito, T. *Inorg. Chim. Acta* **1995**, *228*, 133.
(8) Bernhardt, P. V.; Comba, P.; Hambley, T. W.; Massoud, S. S.; Stebler, S. *Inorg. Chem.* **1992**, *31*, 2644.
(9) Hay, R. W.; Bembi, R.; McLaren, F. *Inorg. Chim. Acta* **1981**, *54*, L161. (b) Zhu, S.; Luo, Q.; Shen, M.; Dai, A.; Huang, L. *Polyhedron* **1992**, *11*, 941. (c) Zhu, S.; Luo, Q.; Shen, M.; Huang, L. *Acta Crystallogr., Sect. C* **1992**, *48*, 1926. (d) Gavrish, S. P.; Lampeka, Y. D. *Theor. Exp. Chem. (Engl. Transl.)* **1995**, *31*, 95.

10.1021/ic9807184 CCC: $18.00
Published on Web 03/09/1999

Chart 1

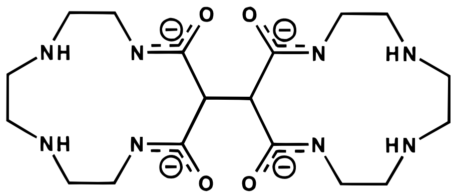

L[1]

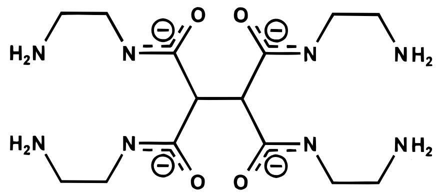

L[2]

Table 1. Crystal Data for $Cu_2L^1 \cdot 14H_2O$ and $Ni_2L^1 \cdot 6H_2O$

	$Cu_2L^1 \cdot 14H_2O$	$Ni_2L^1 \cdot 6H_2O$
empirical formula	$C_{18}H_{58}N_8O_{18}Cu_2$	$C_{18}H_{42}N_8O_{10}Ni_2$
fw	801.79	647.98
cryst sys	monoclinic	monoclinic
space group	$P21/n$ (No. 14)	$C2/c$ (No. 15)
a/Å	8.739(4)	23.505(7)
b/Å	12.140(4)	8.118(7)
c/Å	17.207(4)	15.578(7)
β/deg	103.91(3)	112.52(3)
V/Å^3	1771(1)	2745(2)
Z	2	4
D_{calc}/g cm^{-3}	1.503	1.567
μ(Mo Kα)/cm^{-1}	12.81	14.36
R^a	0.040	0.052
$R_w{}^b$	0.044	0.046

[a] $R = \sum||F_o| - |F_c||/\sum|F_o|$. [b] $R_w = [(\sum w(|F_o| - |F_c|)^2/\sum wF_o{}^2)]^{1/2}$.

Table 2. Selected Bond Distances (Å) and Valence Angles (deg) (Computed Values in Italics) of $Cu_2L^1 \cdot 14H_2O$, $Cu_2L^2 \cdot 10H_2O$,[a] $Ni_2L^1 \cdot 6H_2O$, and Ni_2L^2 [b]

param	$Cu_2L^1 \cdot 14H_2O$	$Cu_2L^2 \cdot 10H_2O^a$	$Ni_2L^1 \cdot 6H_2O$	$Ni_2L^{2\,b}$
M−N(1)	1.930(3)	1.953(2)	1.842(3)	1.865(2)
	1.944	*1.951*	*1.824*	*1.831*
M−N(2)	2.027(3)	2.017(3)	1.907(4)	1.912(3)
	1.985	*2.008*	*1.879*	*1.871*
M−N(3)	2.036(3)	2.023(2)	1.910(4)	1.915(3)
	2.015	*2.009*	*1.898*	*1.879*
M−N(4)	1.929(3)	1.942(3)	1.843(4)	1.867(2)
	1.975	*1.951*	*1.814*	*1.820*
Cu−O(3)	2.301(3)	2.460(3)		
	2.284	*2.363*		
N(1)−M−N(2)	85.6(1)	84.6(1)	88.1(2)	84.3(1)
	84.5	*84.3*	*86.9*	*88.7*
N(2)−M−N(3)	85.8(1)	94.0(1)	88.6(2)	83.8(1)
	86.9	*91.5*	*87.9*	*82.0*
N(3)−M−N(4)	86.0(1)	84.4(1)	86.5(2)	94.7(1)
	85.4	*83.8*	*87.2*	*91.2*
N(1)−M−N(4)	95.3(1)	95.0(1)	96.7(2)	97.2(1)
	95.9	*97.4*	*96.5*	*95.8*
N(1)−M−N(3)	150.9(1)	168.8(1)	176.7(2)	176.6(1)
	146.8	*167.7*	*173.8*	*171.9*
N(2)−M−N(4)	164.4(1)	170.0(1)	166.5(2)	178.3(1)
	167.9	*166.2*	*164.6*	*173.3*
N(1)−Cu−O(3)	110.4(1)	104.8(1)		
	115.6	*102.3*		
N(2)−Cu−O(3)	90.8(1)	89.4(1)		
	91.7	*92.4*		
N(3)−Cu−O(3)	97.4(1)	86.3(1)		
	93.9	*87.7*		
N(4)−Cu−O(3)	103.4(1)	100.3(1)		
	100.6	*98.9*		

[a] Reference 8. [b] Reference 9b.

Results and Discussion

X-ray Structures. The crystallographic data for $Cu_2L^1 \cdot 14H_2O$ and $Ni_2L^1 \cdot 6H_2O$ are given in Table 1, selected bond distances and valence angles are assembled in Table 2, and the molecular structures are shown in Figure 1 (Table 2 and Figure 1 also include information on $Cu_2L^2 \cdot 10H_2O$[8] and Ni_2L^2 [9b]). The structures of $Cu_2L^1 \cdot 14H_2O$, $Cu_2L^2 \cdot 10H_2O$ and Ni_2L^2 are centrosymmetric with a torsion angle ϕ(M−C$_1$−C$'_1$−M$'$) of 180°. $Ni_2L^1 \cdot 6H_2O$ has a folded structure with $\phi = 55°$. The C$_1$−C$'_1$ (bridgehead) distances in all structures are slightly elongated (ca. 1.57 Å). Other structural parameters, including metal donor distances and coordination geometries, are as expected (Table 2). The dicopper(II) compounds are square pyramidal with axial water ligands at 2.30 and 2.46 Å for $Cu_2L^1(OH_2)_2$ and $Cu_2L^2(OH_2)_2$, respectively, while the dinickel(II) compounds are square planar. As expected, due to the relatively small macrocyclic ring (13-membered), there is a considerable distortion of the CuN_4 chromophores from planarity (planar, $\theta = 0°$; tetrahedral, $\theta = 90°$; $\theta = 39°$ for $Cu_2L^1(OH_2)_2$, $\theta = 16°$ for $Cu_2L^2(OH_2)_2$); the dinickel(II) chromophores are less distorted ($\theta = 13°$ for Ni_2L^1, $\theta = 3°$ for Ni_2L^2). Due to the planarity of the coordinated (deprotonated) amide donors, the distortion of the MN_4 planes, and the M−N$_{amide}$ distances, there are significant differences in the geometries of the six-membered chelate rings. While these are practically planar for the dinickel(II) complexes, they are puckered in the dicopper(II) compounds. There is a twist of the carbonyl atoms out of the N_4 planes: $\theta'(N_4/R_2CO)$; $\theta'(Cu_2L^1(OH_2)_2) = 30°$; $\theta'(Cu_2L^2(OH_2)_2) = 28°$; $\theta'(Ni_2L^1) = 15°$; $\theta'(Ni_2L^2) = 27°$. In the two dicopper(II) structures the orientation of the carbonyl oxygen is exo to the axial water ligands (see Figure 1). This might explain why, in both dicopper(II) structures, the axial donors are endo to the second copper(II) site (see model calculations below).

Solution Structure of $Cu_2L^1(OH_2)_2$. The combination of force field calculations with the simulation of various properties (spectroscopy, redox potentials, isomer distributions) has been used to determine structures of coordination compounds in solution.[10] The refinement of structures in solution is of importance when crystal structures are not available and/or when the compound undergoes structural changes upon dissolution, as is often the case with labile copper(II) compounds. There are small differences in the EPR spectra of the dicopper(II) complexes of the bismacrocyclic ligand L^1 and the parent open-chained ligand L^2,[8] and it was of interest to relate these differences to the corresponding solution structures.

The EPR spectrum of $Cu_2L^1(OH_2)_2$ in frozen methanolic solution (Figure 2) is typical for a dipolar interaction between the copper(II) ions, with $A_{||}$ approximately half of that of the corresponding mononuclear compound, as expected for highly delocalized electrons. The spin Hamiltonian parameters $g_{||} = 2.300$, $g_\perp = 2.053$, $A_{||} = 102 \times 10^{-4}$ cm^{-1}, $A_\perp = 32 \times 10^{-4}$ cm^{-1} were obtained from the simulation of the EPR spectrum, assuming that both copper(II) sites are identical and have approximately axial symmetry. The structural parameters obtained from the simulation of the spectrum and from the strain energy minimized structure are assembled in Table 3, where

(10) (a) Comba, P. *Coord. Chem. Rev.* **1993**, *123*, 1. (b) Comba, P. *Comments Inorg. Chem.* **1994**, *16*, 133. Comba, P. In *Fundamental Principles of Molecular Modeling*; Gans, W., Amann, A., Boeyens, J. C. A., Eds.; Plenum Press: New York, 1996.

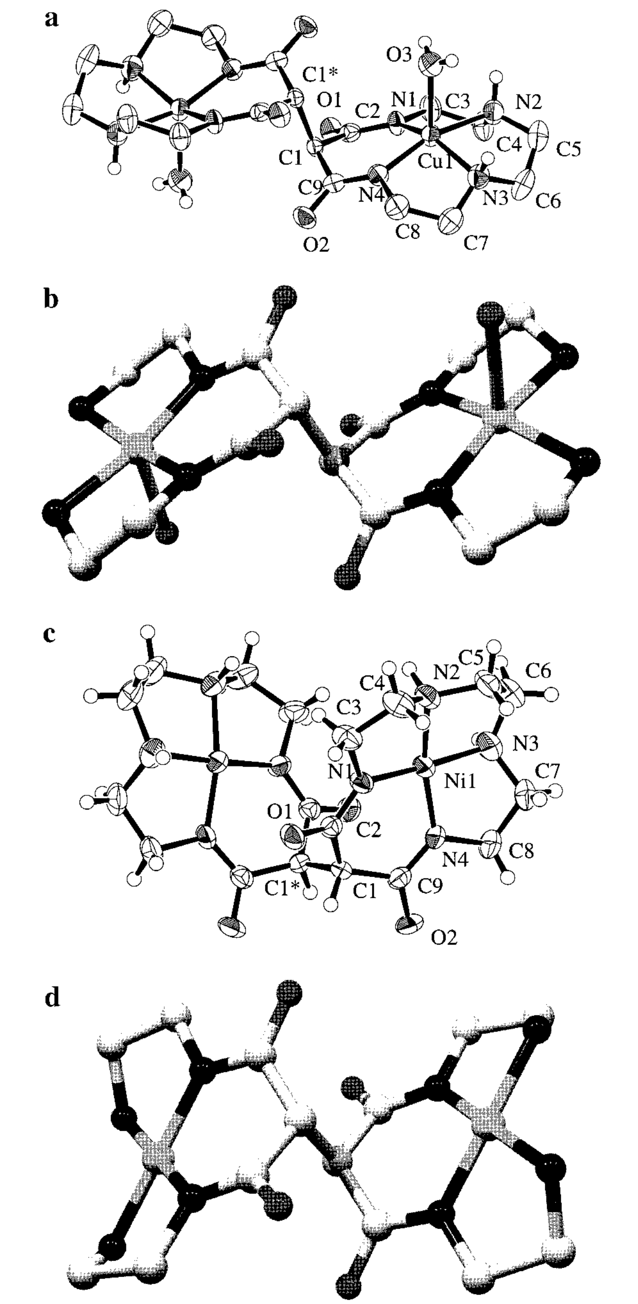

Figure 1. Perspective drawing of the complexes (a) $Cu_2L^1 \cdot 14H_2O$, (b) $Cu_2L^2 \cdot 14H_2O$, (c) $Ni_2L^1 \cdot 6H_2O$, and (d) Ni_2L^2 (atom-numbering schemes and thermal vibrational ellipsoids are given for the structures reported here (a,c); C−H hydrogens are omitted, with the exception of (c), for clarity).

the corresponding parameters of the X-ray structure of $Cu_2L^1(OH_2)_2$ and those of $Cu_2L^2(OH_2)_2$[8] are also tabulated.

The structural parameters of $Cu_2L^1(OH_2)_2$ in solution are, as expected, similar to those in the solid state. The small differences observed may be due to (i) structural differences between the solid state and solution structures, supported by slightly different energies of the d−d transition (17 500 and 18 000 cm^{-1} for the solid and the solution electronic spectra, respectively); (ii) small inconsistencies of the force field parametrization; and (iii) inherent inaccuracies of the spectra simulations (*g*- and *A*-strain are not included). The differences between the predictions based on the structure obtained by the force field optimization and the EPR simulation are partly related to the fact that the simulation of the EPR spectrum is based on the relative

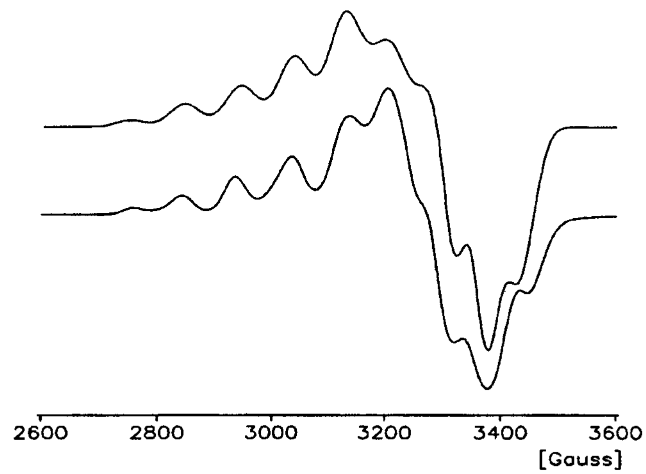

Figure 2. Simulated (top) and experimental (bottom) EPR spectra of $[Cu_2L^1(H_2O)_2]$ (X-band frozen solution, methanol, 120 K).

Table 3. Geometric Parameters for $Cu_2L^1(OH_2)_2$ (Corresponding Data for $Cu_2L^2(OH_2)_2$[a] in Parentheses)[b]

param	r (Å)	ξ (deg)	τ (deg)	η (deg)
X-ray	6.83 (6.9)	90 (70)	0 (0)	45 (45)
MM (experimentally observed conformer)	6.03 (7.2)	90 (75)	0 (0)	45 (45)
EPR simulation	6.4 (6.7)	84 (67)	0 (0)	45 (45)

[a] Reference 8. [b] r is $Cu_1{-}Cu_2$ distance, ξ is the angle between the z-axis of the tensor of Cu_1 and the $Cu_1{-}Cu_2$ vector, τ is the angle between the z-axes of the **g** tensors of Cu_1 and Cu_2, and η is the angle between the y-axis of the **g** tensor of Cu_1 and the $Cu_1{-}Cu_2$ vector, transformed to the xy-plane of Cu_1.[8]

orientation of the **g** tensors of the two copper(II) sites which might be slightly misaligned with respect to the molecular coordinate system.

The $g_{||}$ value of 2.30 is rather high for a planar tetracoordinate copper(II) chromophore[11] (the related mononuclear compound has a $g_{||}$ value of 2.18[12]), indicating a considerable distortion.[11−15] This is consistent with comparably small $A_{||}$ hyperfine constants for the dinuclear compound ($2A_{||} = 204 \times 10^{-4}$ cm^{-1} vs $A_{||} = 222 \times 10^{-4}$ cm^{-1} for the parent mononuclear compound) and with a rather large difference in the d−d transition energies of the solution spectra (18 000 cm^{-1} for Cu_2L^1 vs 19 200 cm^{-1} for the corresponding mononuclear compound).[12] The crystal structure of the parent mononuclear compound has not been reported, but reflectance spectra suggest that a considerable structural difference between these compounds remains also in the solid state ($\nu_{max} = 18\,200$ and 17 500 cm^{-1} for the mono- and dinuclear compounds, respectively).

Model Calculations. The geometries of the four dinuclear compounds were optimized with molecular mechanics. For the two dicopper(II) compounds there are, on the basis of the relative orientations of the axial water ligands, three possible geometries each, i.e., endo-endo, endo-exo, and exo-exo (see Figure 3; the solid state structures have endo-endo geometry, see Figure 1a,b). For the macrocyclic ligand complexes $Cu_2L^1(OH_2)_2$ and Ni_2L^1 the configurations of the coordinated amine donors (*S*) or *R*) are another source of isomerism, and for each isomer of the macrocyclic ligand complexes $Cu_2L^1(OH_2)_2$ and Ni_2L^1 there are

(11) Comba, P.; Hambley, T. W.; Hitchman, M. A.; Stratemeier, H. *Inorg. Chem.* **1995**, *34*, 3903.
(12) Lampeka, Y. D.; Gavrish, S. P. *J. Coord. Chem.* **1990**, *21*, 351.
(13) Comba, P.; Hilfenhaus, P.; Nuber, B. *Helv. Chim. Acta* **1997**, *80*, 1831.
(14) Hathaway, B. J. In *Comprehensive Coordination Chemistry*; Wilkinson, G., Ed.; Pergamon Press: Oxford, 1987.
(15) McGarvey, B. R. *Transition Met. Chem.* **1966**, *3*, 89.

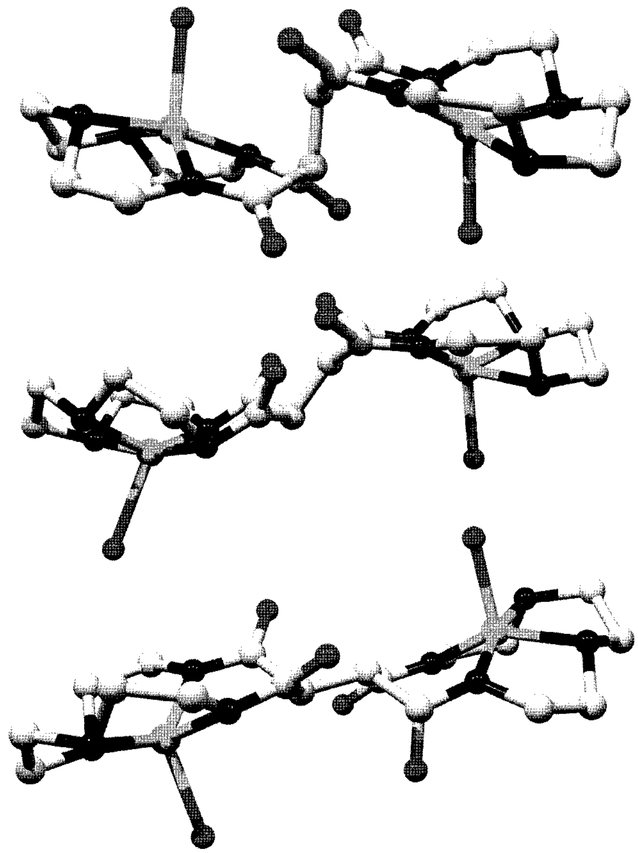

Figure 3. Plots of the strain energy optimized structures (lowest energy conformers) of *endo-endo-*, *endo-exo-*, and *exo-exo-*$[Cu_2L^1(OH_2)_2]$ (top to bottom).

six five-membered chelate rings (λ or δ conformation); for the compounds with the open-chained ligand L^2 there are four. It follows that for the dinuclear copper(II) compounds with the macrocyclic ligand L^1 there are 468 nondegenerate conformations. That observed in the solid state is *endo-endo-*$[Cu_2(S)$-(R)-$\lambda\lambda\delta\lambda\lambda\delta$-$L^1(OH_2)_2]$ (consecutive numbering of configurations and conformations; for atom-numbering scheme, see Figure 1a). For the corresponding Ni_2L^1, $Cu_2L^2(OH_2)_2$, and Ni_2L^2 complexes there are 117, 52, and 13 possible conformers, respectively. The most stable geometries of $Cu_2L^1(OH_2)_2$ and Ni_2L^1 are assembled in Table 4. The conformational analysis involved a search protocol that excluded different conformational patterns at the two metal sites. Inversion at an amine donor leads to a loss of energy of approximately 20 kJ/mol (see lower part of Table 4); these high-energy structures were excluded from the full conformational analysis. The analysis of $Cu_2L^2(OH_2)_2$ and Ni_2L^2 leads to similar results. From the computed structures and strain energies it emerges that, for all four compounds discussed here, the crystallographically observed structures are those of lowest energy but there is only a relatively small energy gap to the next stable conformers.

The preferred relative orientation of the two chromophores in $Cu_2L^1(OH_2)_2$, Ni_2L^1, $Cu_2L^2(OH_2)_2$, and Ni_2L^2 was analyzed by monitoring the strain energies of all low-energy conformers as a function of the torsional angles ϕ ($M-C_{bridgehead}-C'_{bridgehead}-M'$; see Figures 4, 5, and 6; the plots shown are those of the lowest strain energy structures each). These curves were obtained by constraining the torsional angles ϕ to specific values and varying them in 5° intervals between 0° and 180°. Since some of these plots compare nonisomeric structures, the emerging strain energies have all been normalized to obtain zero strain at the fully stretched forms (ϕ = 180°).

Table 4. Strain Energies of All Low-Energy Conformations of Cu_2L^1 and Ni_2L^1 [a]

confomer	strain energy (kJ/mol) (ϕ(M−C$_1$−C$_1$′−M′) (deg))	
(*S*)(*R*)-$\lambda\lambda\lambda\lambda\lambda\lambda$-$Cu_2L^1$	70 (180)	85 (65)
(*S*)(*R*)-$\lambda\lambda\delta\lambda\lambda\delta$-$Cu_2L^1$	61 (180)	79 (70)
(*S*)(*R*)-$\lambda\delta\lambda\lambda\delta\lambda$-$Cu_2L^1$	65 (180)	79 (70)
(*S*)(*R*)-$\delta\lambda\delta\delta\lambda\delta$-$Cu_2L^1$	62 (180)	79 (70)
(*S*)(*R*)-$\delta\delta\lambda\delta\delta\lambda$-$Cu_2L^1$	70 (180)	79 (70)
(*S*)(*R*)-$\delta\delta\delta\delta\delta\delta$-$Cu_2L^1$	70 (180)	80 (75)
(*S*)(*R*)-$\lambda\lambda\lambda\lambda\lambda\lambda$-$Ni_2L^1$	131 (55)	139 (180)
(*S*)(*R*)-$\lambda\lambda\delta\lambda\lambda\delta$-$Ni_2L^1$	106 (55)	125 (180)
(*S*)(*R*)-$\lambda\delta\lambda\lambda\delta\lambda$-$Ni_2L^1$	114 (55)	115 (180)
(*S*)(*R*)-$\delta\lambda\delta\delta\lambda\delta$-$Ni_2L^1$	112 (55)	110 (180)
(*S*)(*R*)-$\delta\delta\lambda\delta\delta\lambda$-$Ni_2L^1$	135 (55)	141 (180)
(*S*)(*R*)-$\delta\delta\delta\delta\delta\delta$-$Ni_2L^1$	119 (55)	121 (180)

conformer	strain energy (kJ/mol) (ϕ(M−C$_1$−C$_1$′−M′) (deg))
(*S*)(*R*)-$\lambda\lambda\delta\lambda\lambda\delta$-$Cu_2L^1$	61 (180)
(*S*)(*S*)-$\lambda\lambda\delta\lambda\lambda\delta$-$Cu_2L^1$	87 (180)
(*R*)(*R*)-$\lambda\lambda\delta\lambda\lambda\delta$-$Cu_2L^1$	89 (180)
(*S*)(*R*)-$\lambda\lambda\delta\lambda\lambda\delta$-$Ni_2L^1$	106 (55)
(*S*)(*S*)-$\lambda\lambda\delta\lambda\lambda\delta$-$Ni_2L^1$	125 (55)
(*R*)(*R*)-$\lambda\lambda\delta\lambda\lambda\delta$-$Ni_2L^1$	120 (55)

[a] Only endo-endo isomers are tabulated for the dicopper(II) compounds; see text for the nomenclature of the conformers.

With the bismacrocyclic ligand L^1 (Figure 4) the dinickel(II) compound with a folded structure (ϕ = 55°) is more stable by approximately 20 kJ/mol than the stretched form with ϕ = 180°. A detailed analysis of all energy terms indicates that attractive van der Waals forces involving the ligand backbone are responsible for this result. $Cu_2L^1(OH_2)_2$ also has a local energy minimum at approximately 55°, but the folded structure is less stable than the stretched isomer by approximately 20 kJ/mol. At ϕ = 120° there is a strain energy maximum for the dicopper(II) and the dinickel(II) compounds, which is due to van der Waals repulsion in this eclipsed conformation. For the three compounds the energy barrier is of the same order of magnitude, i.e., approximately 25 kJ/mol, and the stability difference beween the two rotamers (stretched and folded) is, for the two relevant compounds ($Cu_2L^1(OH_2)_2$ and Ni_2L^1), approximately 20 kJ/mol each. That is, for both compounds only one isomer (that observed in the solid state and, for the dicopper(II) species, also in solution) is expected to be stable in solution.

Since the axial water ligands might be of importance for the geometric preference of $Cu_2L^1(OH_2)_2$, the lowest energy conformer of each of the three isomers (endo-endo, endo-exo, exo-exo; see Figure 3) was analyzed by a strain energy versus torsional angle ϕ plot. These are shown in Figure 5. For each of the three isomers the stretched geometry is preferred by approximately 10−20 kJ/mol. Note that the relative energies of the stretched structures are 0, 7, and 14 kJ/mol for the endo-endo, endo-exo, and exo-exo forms, respectively. That is, the experimental observation that only one isomer, *endo-endo-*$[Cu_2(S)(R)$-$\lambda\lambda\delta\lambda\lambda\delta$-$L^1(OH_2)_2]$, is present in the solid state and in solution is confirmed by these model calculations. The destabilization of the exo forms may be related to the puckering of the six-membered chelate rings (see Figures 1 and 5) that leads to repulsive interactions involving the amide oxygen atoms.

The strain energy versus torsional angle ϕ plots of the two complexes with the open-chained ligand ($Cu_2L^2(OH_2)_2$ and Ni_2L^2) are presented in Figure 6. With this ligand, both the dicopper(II) and the dinickel(II) compounds prefer the stretched

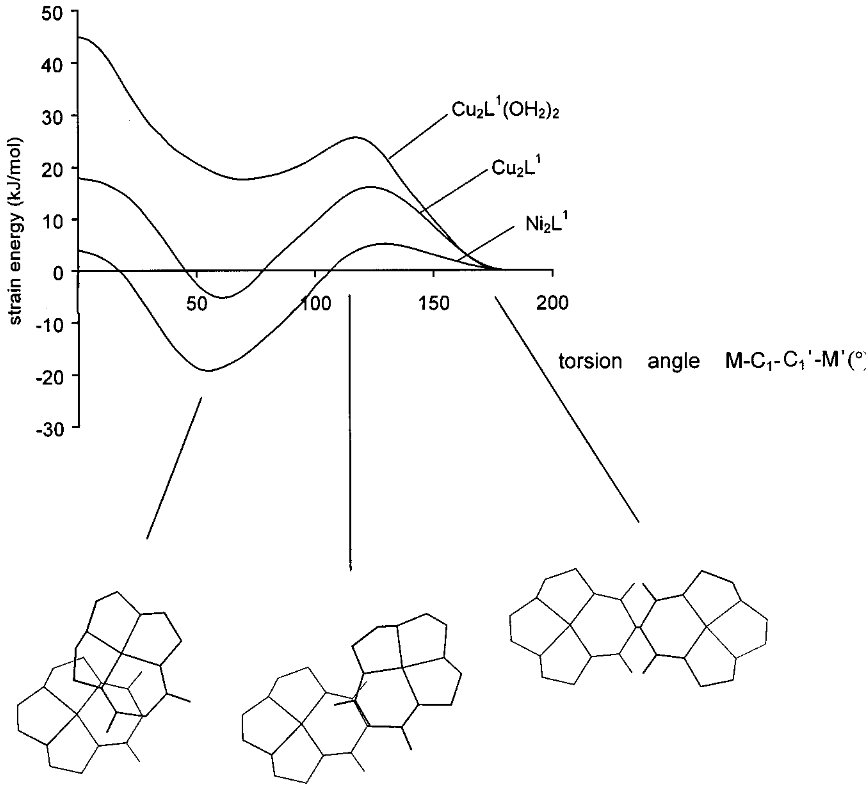

Figure 4. Strain energy versus torsional angle plots ($\phi = M-C_1-C_1'-M'$) of the dicopper(II) compound (with and without axial ligands) and of the dinickel(II) compound of the bismacrocyclic ligand L^1.

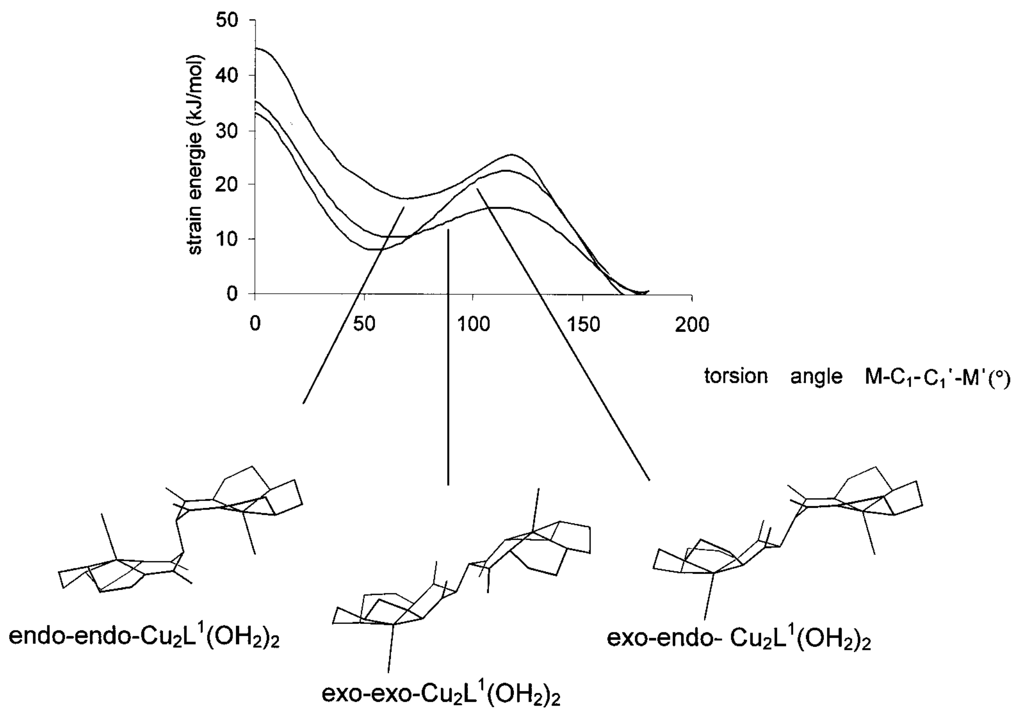

Figure 5. Strain energy versus torsional angle plots ($\phi = M-C_1-C_1'-M'$) of the three isomers (endo-endo, endo-exo, and exo-exo) of the dicopper(II) compound of the bismacrocyclic ligand L^1.

geometry. This is in agreement with the experimentally observed structures and, for the dicopper(II) compound, also with the solution structure. However, the relatively small energy difference of approximately 5 kJ/mol for Ni_2L^2 indicates that, in solution, there might be a dynamic equilibrium (activation energy of approximately 20 kJ/mol) between the two forms. The analysis of all strain energy terms of the two forms of Ni_2L^1 and Ni_2L^2 indicates that the striking structural differences are based on attractive van der Waals terms involving the central five-membered chelate ring.

Experimental Section

The UV–vis and IR spectra were measured on a Specord M40 and a Specord 75IR (Carl Zeiss) instrument, respectively. EPR spectra were recorded on a Bruker ESP300E spectrometer (9.4635 GHz) as approximately 1 mmol dm^{-3} frozen solutions in methanol at 120 K. The

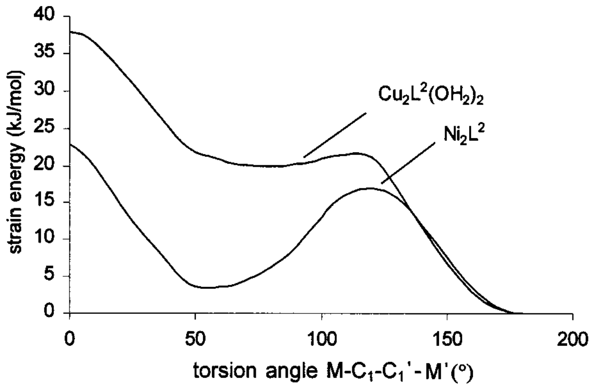

Figure 6. Strain energy versus torsional angle plots (ϕ = M−C_1−C_1′−M′) of the dicopper(II) compound (with axial ligands) and of the dinickel(II) compound of the open-chained ligand L^2.

Table 5. New Force Field Parameters for (4 + 1)-Coordinate Copper(II) and Four-Coordinate Nickel(II) Compounds with Amide/Amine Donors[a,b]

Bond Distance Parameters

bond type	force constant (mdyn Å^{-1})	strain-free bond distance (Å)
Ni−N_{amine}	0.60	1.83

Valence Angle Parameters

valence angle type	force constant (mdyn Å rad^{-2})	strain-free valence angle (rad)
N_{amine}−Ni−N_{amide}	0.025	1.571
N_{amine}−Ni−N_{amine}	0.025	1.571
Ni−N_{amine}−C_{carbon}	0.200	1.920
Ni−N_{amide}−C_{carbon}	0.200	2.094
Ni−N_{amide}−$C_{carboxyl}$	0.200	2.094
Ni−N_{amine}−H	0.100	1.915
N_{amine}−Cu−O	0.007	1.571
N_{amide}−Cu−O	0.007	1.571

Torsion Angle Parameters

bond torsional angle type	force constant (mdyn Å)	offset angle (rad)
N_{amine}−Ni	0.00	2.094
N_{amide}−Ni	0.00	2.094
Cu−O	0.00	2.094
N_{amine}−Cu	0.00	2.094
N_{amide}−Cu	0.00	2.094

[a] All other parameters are given in the literature.[18] [b] dyn = 10^{-5} N.

spin Hamiltonian parameters, the copper−copper separation, and the relative orientation of the chromophores of the dipole−dipole coupled dinuclear copper(II) complexes were determined by simulation of the $\Delta M_s = 1$ resonances with the computer program DISSIM.[16] Molecular mechanics calculations were performed with the strain energy minimization program[17] and force field[18] MOMEC. Parameters not reported before are given in Table 5. These have been fitted to all relevant structures obtained from the CCDC (Cambridge Crystallographic Data Centre).

Syntheses. The ligand H_4L^1 was synthesized as described in the literature.[7b] The dicopper(II) complex was obtained from an aqueous solution (100 cm^3, pH 7, NaOH) of 0.4 g of H_4L^1 and 0.7 g of Cu(ClO_4)$_2$·6H_2O. The solution was filtered and stored in a refrigerator. The blue precipitate was collected on a filter, washed with ethanol and ether, and air-dried. Concentration of the solution to 30 cm^3 yielded an additional crop of the product. Yield: 0.34 g, 47%. Found: C, 26.9; H, 7.4; N, 14.1. Calcd for $C_{18}H_{58}N_8Cu_2O_{18}$: C, 27.0; H, 7.3; N, 14. Vis (H_2O): ν_{max} = 18 000 cm^{-1}, ϵ = 150 dm^3 mol^{-1} cm^{-1} per copper(II); reflectance spectrum, ν_{max} = 17 500 cm^{-1}. IR (KBr pellet): ν_{max} = 1585 cm^{-1} (C═O). The dinickel(II) complex was synthesized from an aqueous solution (50 cm^3, pH 8, NaOH) of 0.2 g of H_4L^1 and 0.23 g of Ni($OOCCH_3$)$_2$·4H_2O. The yellow precipitate which was obtained after evaporation of the resulting solution to 1 cm^3 was filtered and washed with ethanol. Yield: 0.19 g (62%). Found: C, 33.2; H, 6.6; N, 17.2. Calcd for $C_{18}H_{42}N_8O_{10}Ni_2$: C, 33.3; H, 6.5; N, 17.3. Vis (H_2O): ν_{max} = 23 200 cm^{-1}, ϵ = 64 dm^3 mol^{-1} cm^{-1} per nickel ion. IR (KBr pellet): ν_{max} = 1580 cm^{-1} (CO). Crystals suitable for X-ray analyses were obtained by slow diffusion of acetone into an aqueous solution of the complex.

Crystal Structure Determination. Data Collection and Processing. The crystals were mounted on glass fibers. All measurements were made on a Rigaku AFC7S diffractometer with graphite-monochromated Mo Kα radiation (λ = 0.710 69 Å). The data were collected at a temperature of 293 ± 1 K using the $\omega-2\theta$ scan technique to a maximum 2θ value of 50.0°. The intensities of three representative reflections were measured after every 150 reflections. No decay correction was applied, and the data were corrected for Lorentz and polarization effects.

Structure Solution and Refinement. The structures were solved by direct methods[19] and expanded using Fourier techniques.[20] The non-hydrogen atoms were refined anisotropically. Hydrogen atoms of the water molecules were refined isotropically, and the other hydrogen atoms were included at fixed positions. All calculations were performed using the teXsan crystallographic software package.[21]

Detailed information on the X-ray structure analyses is available from the CCDC (Cambridge Crystallographic Data Centre).

Acknowledgment. Generous financial support by the German Science Foundation (DFG), the Bundesministerium für Bildung und Forschung (BMBF), and the Fonds der Chemischen Industrie (FCI) is gratefully acknowledged. This project has also been supported by the Royal Society of Chemistry and the Foundation of Basic Research, the Department of International Cooperation of the Ministry of the Ukraine for Science and Technology, the St. Leonards College at the University of St. Andrews, and a grant from the Royal Society Joint Projects with the former Soviet Union.

Supporting Information Available: Two X-ray crystallographic files, in CIF format, are available. This material is available free of charge via the Internet at http://pubs.acs.org.

IC9807184

(16) Smith, T. D.; Pilbrow, J. R. *Coord. Chem. Rev.* **1974**, *13*, 173.
(17) Comba, P.; Hambley, T. W.; Lauer, G.; Okon, N. *MOMEC97, a molecular mechanics program for coordination compounds adapted to HyperChem*; CVS Heidelberg: e-mail, CVS-HD@T-online.de, 1997.
(18) (a) Bernhardt, P. V.; Comba, P. *Inorg. Chem.* **1992**, *31*, 2638. (b) Comba, P.; Hambley, T. W.; Ströhle, M. *Helv. Chim. Acta* **1995**, *78*, 2042. (c) Bol, J. J.; Buning, C.; Comba, P.; Reedijk, J. *J. Comput. Chem.* **1998**, *19*, 512.
(19) Altomare, A.; Cascarano, G.; Giacovazzo, C.; Guagliardi, A. SIR92. *J. Appl. Crystallogr.* **1993**, *26*, 343.
(20) Beurskens, P. T.; Admiraal, G.; Beurskens, G.; Bosman, W. P.; de Gelder, R.; Israel, R.; Smith, G. M. M. The DIRDIF-94 program system. Technical Report of the Crystallography Laboratory, University of Nijmegen: Nijmegen, The Netherlands, 1994.
(21) *TeXsan: Crystal Structure Analysis Package*; Molecular Structure Corporation: The Woodlands, TX, 1995.